

Available online at www.sciencedirect.com**ScienceDirect**

Nuclear Physics A 982 (2019) 595–598

www.elsevier.com/locate/nuclphysa

XXVIIth International Conference on Ultrarelativistic Nucleus-Nucleus Collisions
(Quark Matter 2018)

Photon-tagged measurements of jet quenching with ATLAS

Dennis V. Perepelitsa, on behalf of the ATLAS Collaboration

University of Colorado Boulder, Boulder, CO 80309 USA

Abstract

Events containing a high transverse momentum (p_T) prompt photon offer a useful way to study the dynamics of the hot, dense medium produced in heavy ion collisions. Because photons do not carry color charge, they are unaffected by the medium, and thus provide information about the momentum, direction, and flavor (quark or gluon) of the associated hard-scattered parton before it begins to shower and become quenched. In particular, the presence of a high- p_T photon can be used to select pp and Pb+Pb events with the same configuration before quenching, limiting the effects of quenching-induced selection biases present in other jet measurements. The large statistics pp and Pb+Pb data delivered by the LHC in 2015 allow for a detailed study of photon-tagged jet quenching effects, such as the overall parton energy loss and modified structure of the component of the shower which remains correlated with the initial parton direction (e.g. in cone). In this proceeding, photon-tagged measurements of jet quenching by ATLAS are reported.

Keywords: heavy ion collisions, quark-gluon plasma, parton energy loss, jet quenching, jet fragmentation

1. Introduction

Photon-tagged measurements of jet energy loss and modification exploit the fact that the outgoing photon is unmodified by its passage through the hot nuclear medium created in Pb+Pb collisions. The large luminosities of Pb+Pb and pp collision data delivered by the LHC in 2015 has enabled a series of high-statistics measurements in these events. These include measurements sensitive to the absolute amount of energy lost outside of a fixed jet cone radius, to how jet structure and substructure are modified, and to where the lost energy or the medium response is distributed in angular and momentum space.

In this proceeding, the first two photon-tagged jet quenching measurements in ATLAS are discussed [1, 2]. A particular focus is the correction for finite resolution effects on kinematic quantities, resulting in distributions reported at the final-state particle level. Because of this improvement, the data can be compared directly for the first time to other data, the predictions of event generators, or models.

2. ATLAS detector and event reconstruction

The measurements summarized here utilize multiple aspects of the ATLAS detector, including the full electromagnetic and hadronic calorimeter systems, the inner detector, and the high-level trigger system. A

<https://doi.org/10.1016/j.nuclphysa.2018.09.056>

0375-9474/© 2018 Published by Elsevier B.V.

This is an open access article under the CC BY-NC-ND license (<http://creativecommons.org/licenses/by-nc-nd/4.0/>).

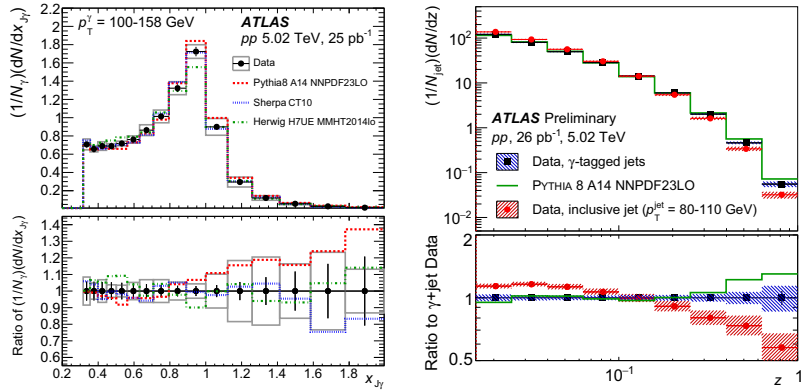


Fig. 1. Measurements in pp collisions of the photon-jet p_T balance (left, from Ref. [1]) and photon-tagged jet FF (right, from Ref. [2]), compared with the analogous distributions in event generators.

detailed description of the detector can be found in Ref. [3]. For both measurements, pp and Pb+Pb events are selected for analysis via the presence of a high- p_T photon in the high-level trigger, which is unpre-scaled and fully efficient for the kinematic range presented here. The centrality of events is characterized by the sum of the transverse energy in both forward calorimeter modules, situated at pseudorapidity $|\eta| = 3.1$ –4.9.

Jets are reconstructed by applying the anti- k_t algorithm with $R = 0.4$ to energy deposits arranged into $\Delta\eta \times \Delta\phi = 0.1 \times 0.1$ logical towers in the calorimeter system. The jet reconstruction procedure features an iterative estimation and subtraction of the underlying event (UE) contribution to each tower. This estimate is performed event-by-event, in a pseudorapidity- and layer-dependent manner, and includes the effects of UE modulation from flow. The measured jet kinematics are calibrated using multiplicative factors based on simulation and on data-to-simulation comparisons of the *in situ* photon/Z+jet balance in pp collisions. More information on jet reconstruction and performance in Run 2 heavy ion data may be found in Ref. [4].

Photon candidates are formed from calorimeter clusters according to the procedure used in proton–proton collisions, but operating on calorimeter cells after UE subtraction. They are required to pass a series of selection cuts on calorimetric shower shapes. Photons are furthermore required to be experimentally isolated via the sum of the transverse energy in calorimeter towers, evaluated after UE subtraction, within a cone of $R = 0.3$ around the photon axis. This value, E_T^{iso} , is required to be smaller than 3 GeV (10 GeV) in pp (Pb+Pb) collisions. More information on the photon reconstruction and performance in heavy ion collisions may be found in Ref. [5].

Charged-particle tracks are reconstructed in the inner detector systems, with selection criteria optimized for the high-occupancy heavy ion environment. More details are provided in Ref. [6].

In both analyses summarized below, events are selected for analysis via the presence of identified, isolated photons in the region $|\eta| < 1.37$ or $1.56 < |\eta| < 2.37$. For the p_T -balance analysis, all jets within $|\eta| < 2.8$ are considered, whereas for the fragmentation function (FF) analysis jets are required to lie within $|\eta| < 2.1$ so that charged particles in the jet cone are contained within the tracking acceptance.

3. Photon-jet transverse momentum balance

High- p_T photons are paired inclusively with all jets satisfying $p_T^{\text{jet}} > 31.6$ GeV and an azimuthal separation $\Delta\phi^{\gamma+\text{jet}} > 7\pi/8$, and the jet-to-photon p_T ratio, $x_{j\gamma}$, is recorded. In Pb+Pb collisions, the distributions are first corrected for the presence of combinatoric photon-jet pairs by evaluating the per-photon rate of these pairs in simulated photon-jet events overlaid with minimum bias Pb+Pb data events. In both pp and Pb+Pb events, these distributions are further corrected for the finite purity of the photon selection (which results in an admixture of hadron fragments, typically π^0 decay photons) via a double sideband technique.

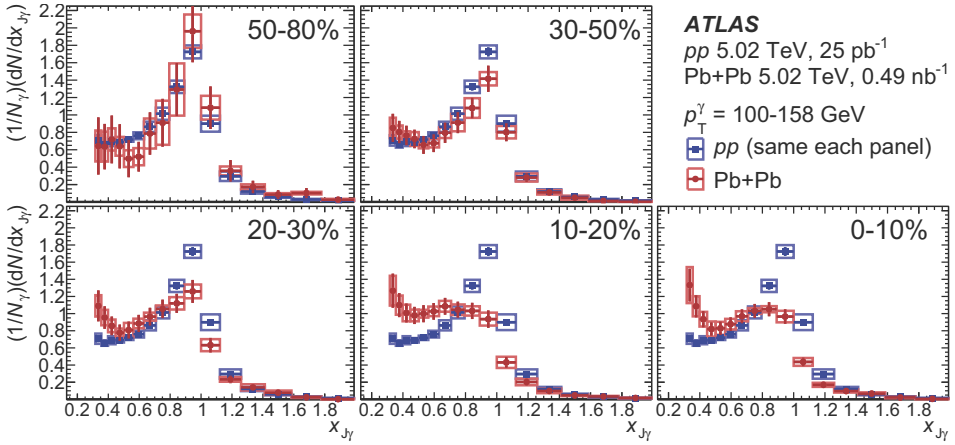


Fig. 2. Comparison of the per-photon jet yield as a function of $x_{J\gamma}$ in Pb+Pb (red, each panel a different centrality selection) and pp collisions (blue), from Ref. [1].

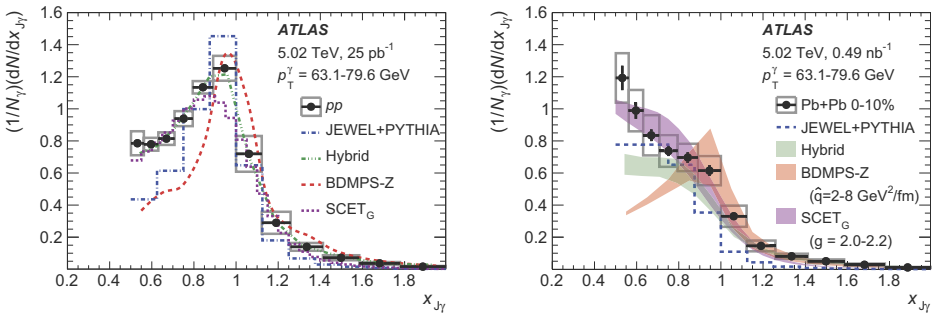


Fig. 3. Example comparisons of fully unfolded $x_{J\gamma}$ results in pp collisions (left) and Pb+Pb collisions (right) to theoretical calculations. See Ref. [1] for further details and references to the theoretical calculations shown here.

The background-subtracted $x_{J\gamma}$ yields are corrected for bin migration and finite efficiency effects via a two-dimensional unfolding procedure similar to that previously used for dijet events in Ref. [7]. After all corrections, $x_{J\gamma}$ distributions are reported in differential selections on the photon p_T and event centrality.

The left panel of Fig. 1 shows the $(1/N_{\gamma})(dN/dx_{J\gamma})$ distribution for one example photon p_T selection in pp collisions, compared to a trio of generator-level predictions from Pythia, Sherpa and Herwig. Correcting for resolution effects recovers a sharp peak in the measured $x_{J\gamma}$ distributions, also observed in event generators, indicative of a strong p_T correlation between photon–jet pairs in pp collisions.

Figure 2 reports the $x_{J\gamma}$ distribution in Pb+Pb events of all centralities for the same photon p_T selection. In peripheral events, the $x_{J\gamma}$ distribution is compatible with that in pp collisions within uncertainties, indicating that energy loss effects are small. In progressively more central events, the $x_{J\gamma}$ distribution is systematically deformed: the mean is shifted to the left, and the yield at small (large) $x_{J\gamma}$ is increased (decreased). Notably, a pp -like peak at $x_{J\gamma} \approx 0.9$ remains even in central collision. This suggests the presence of jets which have lost minimal or no energy and thus remain well-correlated in p_T with the photon.

Figure 3 shows a selected comparison of the data to a suite of energy loss MC models and calculations.

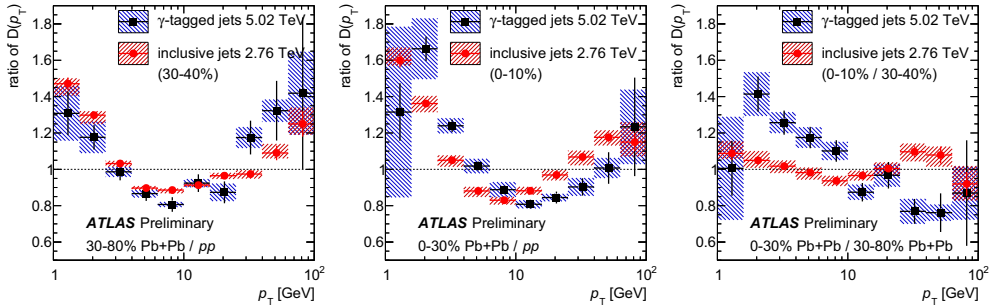


Fig. 4. Ratios of the jet FF as a function of hadron p_T between different event types, comparing photon-tagged jets (black) to inclusively-selected jets (red).

4. Photon-tagged jet fragmentation function

The internal structure of jets with $p_T = 63.1 - 144$ GeV in events with a $p_T = 79.6 - 126$ GeV photon are analyzed. The particular choice of kinematics is used to ensure that only the leading jet opposite to the photon, which is likely to be quark-initiated, enters into the analysis. Corrections are applied for three sources of backgrounds: (1) jets from combinatoric photon-jet pairs entering into the analysis, (2) UE charged particles falling into the jet cone, and (3) hadron fragments reconstructed as photons. These backgrounds are constrained with data-driven methods and subtracted statistically. Bin migration effects are corrected with a two-dimensional unfolding procedure similar to that used in previous FF measurements [6].

The FF for photon-tagged jets in pp collisions is presented as a function of $z = p_T^{\text{hadron}}/p_T^{\text{jet}}$ in the right panel of Fig. 1. It is systematically harder than the analogous quantity for inclusively-selected jets in a similar p_T range, consistent with the expectation from the higher quark-initiated jet fraction.

Figure 4 shows the ratio of the FF between Pb+Pb and pp collisions. In 30–80% events, the FF is modified in a way quantitatively similar to that of inclusive jets. However, in 0–30% central events, the modification is qualitatively different, with additional enhancement (suppression) at low (high) hadron p_T . This stronger centrality dependence is compared to that for inclusive jets in the right panel of Fig. 4.

5. Conclusion

This proceeding briefly summarizes measurements by ATLAS of how photon-tagged jets lose energy and are modified through interactions with the hot nuclear medium created in Pb+Pb collisions. Further information, data, and model comparisons may be found in Refs. [1, 2].

Copyright 2018 CERN for the benefit of the ATLAS Collaboration. CC-BY-4.0 license.

References

- [1] ATLAS Collaboration, Measurement of photon-jet transverse momentum correlations in 5.02 TeV Pb+Pb and pp collisions with ATLAS, arXiv:1809.07280.
- [2] ATLAS Collaboration, Measurement of the fragmentation function for photon-tagged jets in $\sqrt{s_{NN}} = 5.02$ TeV Pb+Pb and pp collisions with the ATLAS detector, ATLAS-CONF-2017-074, Available at <http://cds.cern.ch/record/2285812>.
- [3] ATLAS Collaboration, The ATLAS Experiment at the CERN Large Hadron Collider, JINST 3 (2008) S08003.
- [4] ATLAS Collaboration, Measurement of the nuclear modification factor for inclusive jets in Pb+Pb collisions at $\sqrt{s_{NN}} = 5.02$ TeV with the ATLAS detector, arXiv:1805.05635.
- [5] ATLAS Collaboration, Centrality, rapidity and transverse momentum dependence of isolated prompt photon production in lead-lead collisions at $\sqrt{s_{NN}} = 2.76$ TeV measured with the ATLAS detector, Phys. Rev. C93 (2016) 034914.
- [6] ATLAS Collaboration, Measurement of jet fragmentation in Pb+Pb and pp collisions at $\sqrt{s_{NN}} = 5.02$ TeV with the ATLAS detector, Phys. Rev. C98 (2018) 024908.
- [7] ATLAS Collaboration, Measurement of jet p_T correlations in Pb+Pb and pp collisions at $\sqrt{s_{NN}} = 2.76$ TeV with the ATLAS detector, Phys. Lett. B774 (2017) 379.